A&A 377, 104–112 (2001)
DOI: 10.1051/0004-6361:20011026-1

Astronomy & Astrophysics

Apsidal motion and non-radial pulsations in ψ^2 Ori*

J. H. Telting[1,2], J. B. Abbott[1,3,4], and C. Schrijvers[5,6]

[1] Isaac Newton Group of Telescopes, NWO, Apartado 321, 38700 Santa Cruz de La Palma, Spain
[2] Nordic Optical Telescope, Apartado 474, 38700 Santa Cruz de La Palma, Spain
[3] Division of Physical Sciences, University of Hertfordshire, Hatfield, Hertfordshire AL10 9AB, UK
[4] Department of Physics and Astronomy, University College London, Gower St., London WC1E 6BT, UK
e-mail: jba@star.ucl.ac.uk
[5] Astronomical Institute Anton Pannekoek, University of Amsterdam, and Center for High Energy Astrophysics, Kruislaan 403, 1098 SJ Amsterdam, The Netherlands
[6] Space Department, TNO TPD, Stieltjesweg 1, 2600 AD Delft, The Netherlands
e-mail: schrijvers@tpd.tno.nl

Received 21 March 2001 / Accepted 9 July 2001

Abstract. We present a time series of high-resolution echelle spectra of the double-lined close binary ψ^2 Ori. The spectra sample the wavelength region of 3800–6800 Å. In the absorption lines of the early-B type primary we find clear evidence for non-radial pulsations with intermediate values of the modal degree ℓ. Using a cross-correlation technique we derive the radial velocity of both components. We compare our orbital solution with those reported in the literature to derive the apsidal motion period in this system: 47.5 ± 0.7 year. We analyse the absorption line profiles of the primary using Fourier techniques to derive apparent pulsation periods and ℓ values of two detected modes with apparent frequencies $f_1 = 10.48$ c/d and $f_2 = 10.73$ c/d. We discuss whether the non-radial pulsations in this star are internally excited or due to tidal forcing. Comparing the pulsation frequencies with those expected for tidal forcing and for internally excited modes, we tentatively conclude that these modes are probably due to internally excited β Cephei pulsations.

Key words. stars: early-type – stars: oscillations – line: profiles – binaries: close – binaries: spectroscopic – stars: individual: ψ^2 Ori

1. Introduction

Many early-type B stars are known to show β Cephei like pulsations, which are internally excited due to the κ-mechanism (e.g. Balona & Dziembowski 1999). Waelkens & Rufener (1983) searched for pulsations in photometric observations of close binaries containing early-B type stars, and concluded that for close binaries with periods shorter than that of α Vir (orbital period $P = 4.0$ day, eccentricity $e = 0.15$, pulsations in the primary, Smith 1985) no pulsations are detectable, and argued that in close binaries the tidal forces may suppress the β Cephei pulsations.

In this paper we present spectroscopic detection of multi-frequency non-radial pulsations in the primary of the close binary ψ^2 Ori (HD 35715, $m_V = 4.6$ mag, B1 III + B2 V, $P = 2.5$ day, $e = 0.05$, Lu 1985). In a forthcoming paper (Schrijvers & Telting) on the close binary ν Cen ($P = 2.6$ day, $e = 0.0$) we report an extensive dataset disclosing similar multi-frequency non-radial pulsations. Both these binaries have orbital periods shorter than that of α Vir and have primaries that show β Cephei like pulsations with intermediate values of the pulsational degree ℓ, which could not have been detected photometrically by Waelkens & Rufener (1983).

For ν Cen and α Vir (Smith 1985) there is strong observational evidence that a low-degree (non-)radial mode has damped out. The variable-amplitude low-degree mode in ν Cen (Ashoka & Padmini 1992) which gave rise to a radial velocity amplitude of about 10 km s^{-1} from 1985 to 1988, could not be detected in the high-quality data set, obtained in 1998, to be presented by Schrijvers & Telting. However, as only limited amounts of data of the

Send offprint requests to: J. H. Telting,
e-mail: jht@not.iac.es

* Based on observations made with the Isaac Newton Telescope operated on the island of La Palma by the Isaac Newton Group in the Spanish Observatorio del Roque de los Muchachos of the Instituto de Astrofisica de Canarias.

above stars have been obtained, it is also possible that the apparent low-degree modes and their apparent dissapearance are both observational symptoms of complicated multimodal beating. Nevertheless, it is clear that the conclusion put forward by Waelkens & Rufener (1983) does not hold, but it is still unclear if the tidal forces in close binaries can cause the amplitudes of low-degree β Cephei pulsations to damp out or become variable.

Examples of other close binaries with early-B type components which have shown traces of pulsations are: λ Sco, $P = 6.0$ day, $e = 0.29$, non-radial pulsations in primary (De Mey et al. 1997); β Sco A, $P = 6.8$, $e = 0.29$, non-radial pulsations in secondary (Holmgren et al. 1997); η Ori Aab, $P = 8.0$ day, $e = 0.0$, non-radial pulsations in secondary (De Mey et al. 1996); 16 Lac, $P = 12.1$, $e = 0.047$, radial and non-radial pulsations in primary (Chapellier et al. 1995). The case of ϵ Per, $P = 14$ day, $e = 0.5$, is an intriguing object with well-studied multiperiodic pulsations in the primary (Gies & Kullavanijaya 1988; Tarasov et al. 1995; De Cat et al. 2000).

For the above mentioned close binaries, which all have pulsating components with spectral types in the range of β Cephei stars, another question is important: are the observed pulsations excited internally, or are they powered by the perturbing tidal forces? Witte & Savonije (1999) have shown that tidally excited g- and r-mode oscillations are a means to dissipate orbital energy at large rates, if the disturbing frequency coincides with a resonance frequency of the star. Hence, the study of tidally excited pulsations may have an impact on binary star evolution and on the dynamics of the central parts of globular clusters in which tidal captures of binary components take place.

To study these effects, the case of ψ^2 Ori presents a well-observed system, with a history of orbit determinations of almost a century. This system is known to show rapid apsidal motion (e.g. Batten et al. 1978), and ellipsoidal variations (Percy 1969; Hutchings & Hill 1971; Waelkens & Rufener 1983; Jerzykiewicz 1984), and was labelled as a tentative β Cephei variable by Hill (1967). The luminosity ratio of the primary and secondary is about 4.5 (Lu 1985). The Hipparcos parallax of ψ^2 Ori is 2.3 ± 0.9 mas. Warren & Hesser (1978) list ψ^2 Ori as a member of subgroup 1a of the Orion OB1 association, which has a mean distance of 336 ± 16 pc and an age of 11.4 ± 1.9 Myr (De Zeeuw et al. 1999).

For the binary system ψ^2 Ori, high-resolution time series showing non-radial pulsations have never been presented in the literature before. Of the stars with known β Cephei pulsations in close binaries, ψ^2 Ori is the system with shortest orbital period.

In Sect. 2 we present the data. In Sect. 3 we analyse the radial velocity of the two components of ψ^2 Ori, and determine the geometry of the system. In Sect. 4 we determine and discuss the apsidal motion period of ψ^2 Ori. In Sect. 5 we investigate the line profiles of the primary to derive some of the pulsational characteristics of the star. In Sect. 6 we discuss the possibility that the non-radial pulsations in ψ^2 Ori are due to tidal perturbations.

2. The data

Our 90 high-resolution spectra ($R = 32\,000$) of ψ^2 Ori were obtained on La Palma, with the Isaac Newton Telescope and the fiber-fed ESA-Musicos echelle spectrograph, over a 6 night period (18–24 November 1997) which was mainly free of bad weather. The spectra have a wavelength coverage of about 3800–6800 Å, sampled by 41 echelle orders. The reddest orders are heavily affected by fringing. Most of the spectra were exposed 10 min or less. We discarded 8 spectra from the analysis because of poor count rates.

The spectra were reduced using standard packages in IRAF. The CCD overscan region was used to determine the bias level. One-dimensional spectra were extracted for the individual orders. It was found that pixel-to-pixel variations could not be removed properly using our abundant number of flatfield frames: unflatfielded spectra proved to have better S/N than flatfielded ones. A two-dimensional wavelength solution was obtained from 59 manually selected ThAr calibration lines. Spectra were shifted to, and acquisition times were transformed to, the heliocentric frame. The normalization of the orders was achieved in a way similar to that described by Telting & Schrijvers (1998) in order to minimise variable continuum misplacement in the absorption lines: for each night a spectrum with high S/N was used as a template and was divided into the other spectra of that night. The orders in the resulting quotient spectra were normalized by fitting a high-order cubic spline with typically 10 to 15 spline segments. The templates were normalized with a low-order cubic spline fit to the continuum regions. Then the normalized quotient spectra were transformed back by multiplying with their corresponding normalized template spectrum. The reduced spectra have a typical S/N ratio of between 250 and 450.

In Fig. 1 one can clearly see the orbital variability in the spectra, and the line-profile variations of the primary. We did not detect any significant variations in the line profiles of the secondary.

3. Orbital solution

In order to determine a radial velocity curve for the two components in ψ^2 Ori we used two spectra, in which the stars have a large separation, as templates for cross correlation. In the first template spectrum the primary has a radial velocity of 159 $\mathrm{km\,s^{-1}}$, and -116 $\mathrm{km\,s^{-1}}$ in the second template. For each template we have done a full analysis to obtain an orbital solution; comparison of the two sets of results allows us to estimate the errors of our orbital solution.

For the radial velocity curve of the primary we used 5 echelle orders in the cross-correlation process, covering the following wavelength regions: 4245–4295, 4545–4585, 4562–4615, 4634–4692, and 5010–5055 Å. We used the best 82 spectra for the orbit determination of the primary.

For the secondary we also used 5 orders: 4137–4150, 4382–4395, 4915–4931, 5010–5055, and 5865–5885 Å.

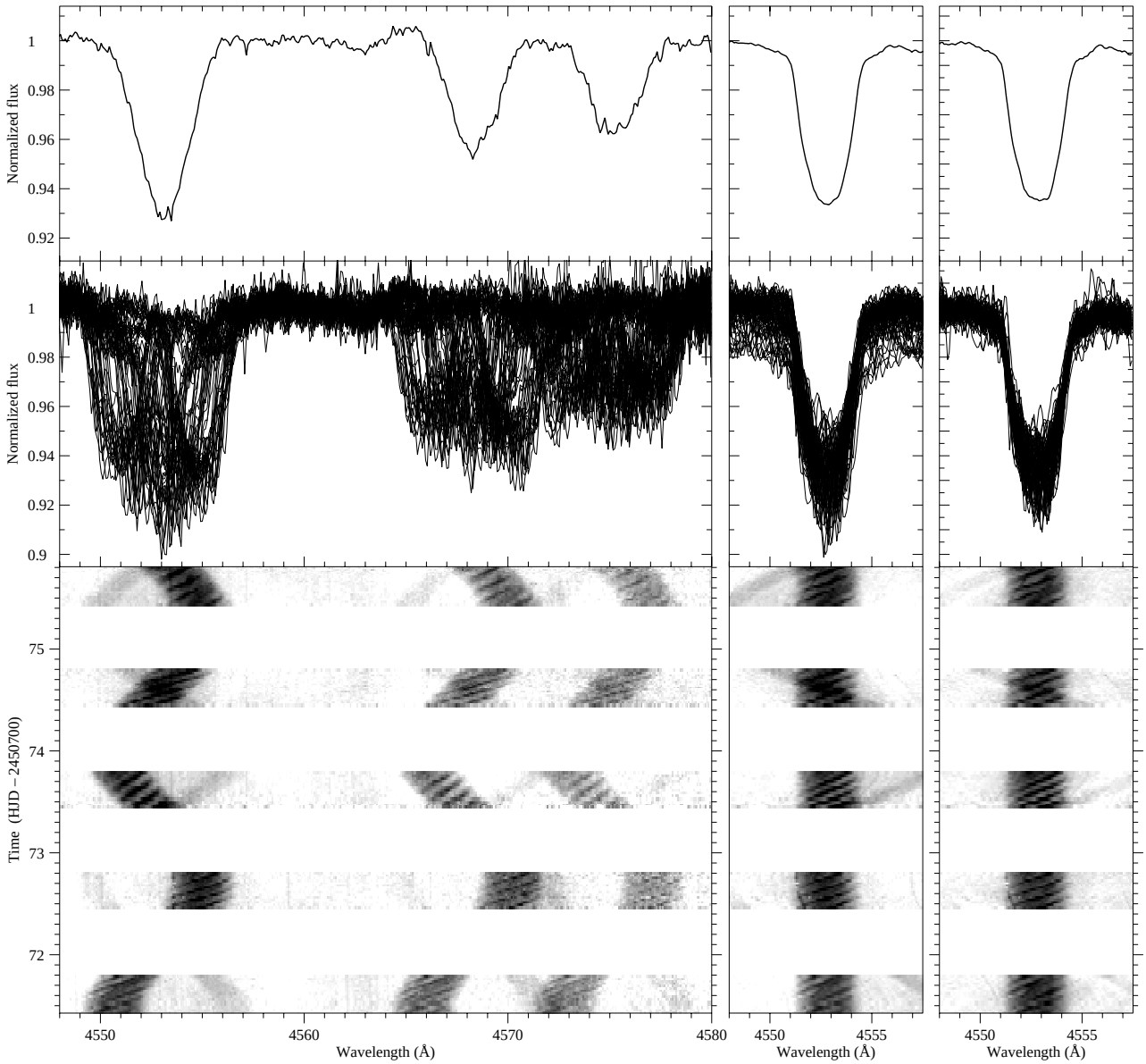

Fig. 1. Left: five nights of data of the SiIII 4552, 4567, and 4574 line profiles. Top: mean of one night. Middle: overplotted spectra. Bottom: grey-scale representation of the spectra, with each spectrum offset according to acquisition time. **Middle:** same for the 4552 profile, but shifted to the velocity frame relative to the primary. The mean of all spectra is plotted in the top panel. **Right:** as middle frame, after prewhitening with the orbital frequency and its first four harmonics to filter out most of the variability caused by the moving profile of the secondary. In the grey-scale plots, moving bumps are clearly visible in the profiles of the primary.

As the weaker lines of the secondary are disturbed by the lines of the primary near conjuctions, we used only 47 spectra for the orbit determination of the secondary.

For each spectrum we used the median radial velocity of the 5 orders. The standard deviation of the 5 values is typically 4 $\mathrm{km\,s^{-1}}$ for the primary, and 12 $\mathrm{km\,s^{-1}}$ for the secondary. We used the error of the mean of the 5 values as error estimates in the orbit fits.

As we did not obtain a useful spectrum of a radial velocity standard, we used the He I lines 4009.27, 4143.76, 4387.93, 4921.93, 5015.68, 5047.74, and 6678.15 Å, to calibrate the velocity shifts of the templates. This resulted in errors in mean for the 7 lines of 4 $\mathrm{km\,s^{-1}}$ and 7 $\mathrm{km\,s^{-1}}$ for primary and secondary respectively. Because of this inaccuracy, our derivation of the system velocity has a similar error.

The radial velocity curve of the two components, and the result of the orbit fits, are plotted in Fig. 2. The results of the fits of the two templates are listed in Table 1. One can see that the differences between the two solutions are larger than the errors of the individual fits allow. Therefore we list an additional final set of orbital parameters, based on the mean values and the error in the mean values of the two solutions. Orbit fits with the period fixed to the value of 2.526 day (Lu 1985) did not give solutions that are significantly different than the ones in Table 1.

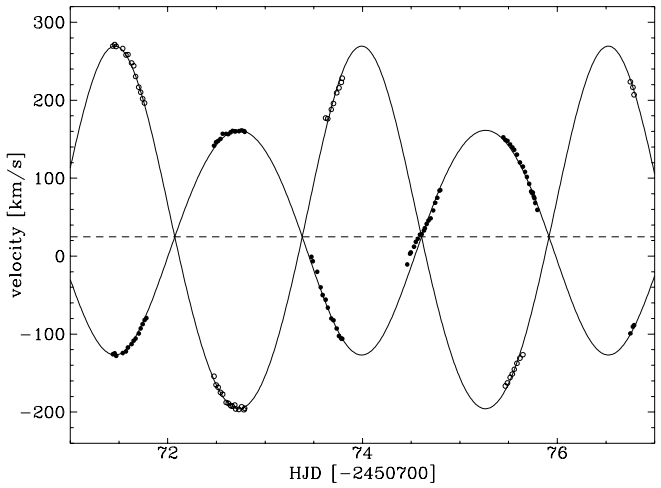

Fig. 2. Orbital solution for the template giving the best χ^2 value (see Table 1). The measured radial velocities of the primary are affected by the profile of the secondary in night 4 of our observations.

3.1. Geometry of the binary system

In order to estimate the radii of the stars in ψ^2 Ori we need an accurate value of their rotational velocities. Lu (1985) has presented estimates of the projected rotational velocity of the two stars of the binary based on the FWHM of He lines: $v_1 \sin i = 95 \pm 5$ km s^{-1} and $v_2 \sin i = 75 \pm 5$ km s^{-1}. We found that the estimate for the primary is somewhat too small to explain the line widths in our spectra. Therefore we fitted a model of a rotating star with pulsations with degree $\ell = 6$ (see Sect. 5) to the mean profile of the spectra of the primary after shifting to the velocity frame relative to the primary (Fig. 1). We fitted the model (Schrijvers et al. 1997) to the Si III 4574 and O II 4590 lines. The derived value of $v_1 \sin i = 105 \pm 6$ km s^{-1} is robust against changes in pulsational parameters, intrinsic line width, and limb darkening. We have checked the previously determined rotation velocity of the secondary, but due to the fact that the lines of heavy elements are very shallow and that the helium lines suffer from normalization problems, we were not able to derive an improved value of $v_2 \sin i$.

Assuming that the rotation rates of the stars are synchronised at periastron ($\Omega^2_{\rm rot} = \frac{(1+e)}{(1-e)^3}\Omega^2_{\rm orb}$, Kopal 1978, i.e. $\Omega_{\rm rot} = 1.11\Omega_{\rm orb}$), and that the stars have aligned their rotation axes perpendicular to the orbital plane, and using the measurements of $v_1 \sin i = 105 \pm 6$ km s^{-1} and $v_2 \sin i = 75 \pm 5$ km s^{-1}, we estimate the equatorial radii of the two components of ψ^2 Ori as $R_1 \sin i = 4.7 \pm 0.3\ R_\odot$ and $R_2 \sin i = 3.3 \pm 0.3\ R_\odot$.

If the assumed rotation rates are correct, and the stars comply to the mass-radius relation for ZAMS stars (Landolt-Börnstein), we can estimate the inclination from the dynamically derived masses in Table 1 and the above radius estimates. The implied inclinations are $i_1 \sim 62°$ for the primary (with 1σ confidence interval $56° \lesssim i_1 \leq 70°$) and $i_2 \sim 65°$ for the secondary ($58° \lesssim i_2 \lesssim 78°$), which are consistent with the orbital inclination $58 \pm 8°$ as derived from light-curve modelling (Hutchings & Hill 1971). Note that the inclination cannot be too large, as no eclipses are observed. (Waelkens & Rufener (1983) present observations hinting at a small eclips, but this observation has never been confirmed.) Taking the estimates $R_1 \sin i = 4.7\ R_\odot$ and $R_2 \sin i = 3.3\ R_\odot$ as polar radii, eclipses are expected for $i \gtrsim 67°$.

With $R_1 \sin i = 4.7 \pm 0.3\ R_\odot$ and $R_2 \sin i = 3.3 \pm 0.3\ R_\odot$, ψ^2 Ori is a detached system with relative radii $R_1/A_1 = 0.66$ and $R_2/A_2 = 0.28$ with respect to the semi-major axes of the orbits, and $R_1/d_1 = 0.45$ and $R_2/d_2 = 0.39$ with respect to the distances d between stellar center and the inner Lagrangian point L_1.

Table 1. Orbital solution. Listed are the results for the two templates, and the mean of these two solutions. The last column lists the number of points used in the fit.

Solution for the first template			
K_1	144.12	0.22	
Eccentricity e	0.0521	0.0011	
Period P	2.5335	0.0013	
Periastron time	2 450 773.967	0.012	
Periastron angle ω	176.1	1.6	
System velocity v_0	24.77	0.17	
K_2	232.57	0.49	
χ^2	574.90		129
rms	5.34		129
rms primary	5.74		82
rms secondary	4.56		47
Solution for the second template			
K_1	145.08	0.19	
Eccentricity e	0.0536	0.0015	
Period P	2.5244	0.0010	
Periastron time	2 450 773.907	0.010	
Periastron angle ω	167.1	1.5	
System velocity v_0	14.01	0.15	
K_2	240.86	0.63	
χ^2	716.18		129
rms	8.43		129
rms primary	4.37		82
rms secondary	12.72		47
Mean values and error in mean			
K_1 [km s^{-1}]	144.6	0.5	
Eccentricity e	0.053	0.001	
Period P [days]	2.529	0.005	
Periastron time [HJD]	2 450 773.94	0.03	
Periastron angle ω [°]	172	5	
System velocity v_0 [km s^{-1}]	19	5	
K_2 [km s^{-1}]	237	4	
$A_1 \sin i$ [10^6 km]	5.02	0.02	
$A_2 \sin i$ [10^6 km]	8.22	0.14	
$m_1 \sin^3 i$ [$M_\odot$]	9.02	0.34	
$m_2 \sin^3 i$ [$M_\odot$]	5.50	0.12	

Table 2. Orbital solutions from the literature.

	JD	orbital period [day]	v_0 [km s^{-1}]	K_1 [km s^{-1}]	K_2 [km s^{-1}]	e	ω [°]	apsidal period [year]
Plaskett (1908)	2 417 916	2.52588	12(1)	144		0.065(0.011)	185(11)	
Beardsley (1969)	2 419 408		17(1)	142		0.05(0.01)	240(15)	
Pearce (1953)	2 429 189	2.52596	16	143	235	0.07	93	
Chopinet (1953)	2 434 024		21(2)	136		0.04(0.02)	221(22)	
Lu (1985)	2 437 685	2.52596	26(1)	139	219	0.044(0.008)	285(14)	
Abt & Levy (1978)	2 442 418		19(1)	142		0.08(0.01)	356(9)	44.8
current	2 450 774	2.529(5)	19(5)	145	237	0.053(0.001)	172(5)	47.5(0.7)

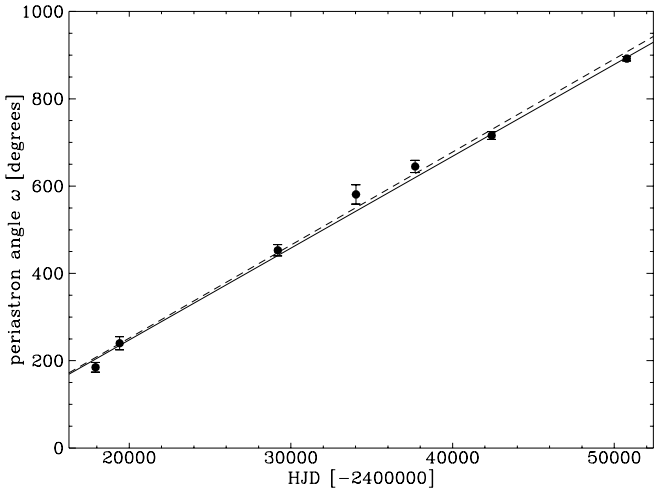

Fig. 3. Apsidal motion: least-squares fit (dashed) and χ^2 fit (solid). See Table 2 for references.

4. Apsidal motion

Table 2 lists the observed values of the periastron angle ω. In Fig. 3 we present a least squares and a χ^2 fit to these data. For the measurement dated JD 2 429 189 we used the average of all other errors on ω as an error estimate. The least squares fit gives for the apsidal motion period $U =$ 46 year, and the χ^2 fit gives $U = 47.5 \pm 0.7$ year. This value is in good agreement with the first estimate by Batten et al. (1978; ∼40 year), and with the value determined by Abt & Levy (1978; 44.8 year). It is in contrast, however, with the value of 149 year determined by Monet (1980).

The observed apsidal motion is due to a not purely Keplerian potential of the binary system. This can be caused by the presence of a third body orbiting ψ^2 Ori, by effects of general relativity, or by tidal and rotational forces in the binary.

As the orbital velocities of the two stars in ψ^2 Ori are mildly relativistic, we can approximate the expected apsidal motion with the expressions given by Giménez (1985) or Stairs et al. (1998). We find that for mass estimates of 13.9 $M_\odot$ and 8.5 $M_\odot$ ($i = 60°$) the period of apsidal motion for this binary expected from the theory of general relativity is about 1000 years. This is in contrast with the observed period of 47.5 year, indicating that other perturbations of the Keplerian potential are more important.

The reported values for the system velocity of ψ^2 Ori range from 12 km s^{-1} to 26 km s^{-1}, which indicates that the value is variable although it is not clear if for all determinations the velocities were transformed to the heliocentric frame. The spread of the points as a function of time does not allow a proper period search in order to find the orbital period of a possible third body. Using Kopal (1959) and Wolf et al. (1999) we find that for a hypothetical $M_3 = 9\ M_\odot$ third component the orbital period P_3 must be as short as about $P_3 \sim 5P = 12.5$ day, in order to give an apsidal motion period similar to that observed. For a less-massive third component, and for a longer orbital period P_3, the apsidal motion period becomes longer ($U \propto P_3^2(M_1+M_2+M_3)/M_3$). It is clear that such a close third body is unlikely and in contrast with the observations of ψ^2 Ori.

We conclude that the observed apsidal motion is due to tidal and rotational forces in this close binary, and that effects of general relativity and a possible third body can be neglected.

4.1. Internal structure constant

Assuming $R_1 \sin i = 4.7 \pm 0.3\ R_\odot$ and $R_2 \sin i = 3.3 \pm 0.3\ R_\odot$, i.e. assuming periastron synchronisation for both components, we computed the internal structure constant as averaged over the two stars, $\overline{k_2}$=$P/(U(c_1+c_2))$, with $c_i \propto (R_i/(A_1+A_2))^5$ as defined in e.g. Claret & Giménez (1993), giving $c_1 = 0.011$ and $c_2 = 0.005$. Neglecting the influences of general relativity and a possible third body we find $\log \overline{k_2} = -2.02 \pm 0.16$. Accounting for general relativity we find $\log \overline{k_2} = -2.00 \pm 0.16$.

We use Tables 17–20 in Claret & Giménez (1992) to compare the observed value of $\overline{k_2}$ with that expected from theory. Using the age of subgroup 1a of the Orion OB1 association, 11.4 ± 1.9 Myr, as the age of the stars in the binary, we find $\log \overline{k_{2,1}} = -2.4$ for the primary and $\log \overline{k_{2,2}} = -2.1$ for the secondary. Combining these numbers with those of c_1 and c_2 leads to a theoretical value of $\log \overline{k_2} = -2.25$. Note that with the adopted age of 11.4 Myr the primary is very near to the end of the main sequence, if it is as massive as 15 $M_\odot$. For this reason the tabulated value of $\log \overline{k_{2,1}}$ is high. The discrepancy between observed and theoretical values of $\log \overline{k_2}$ therefore indicates that the binary is somewhat younger than

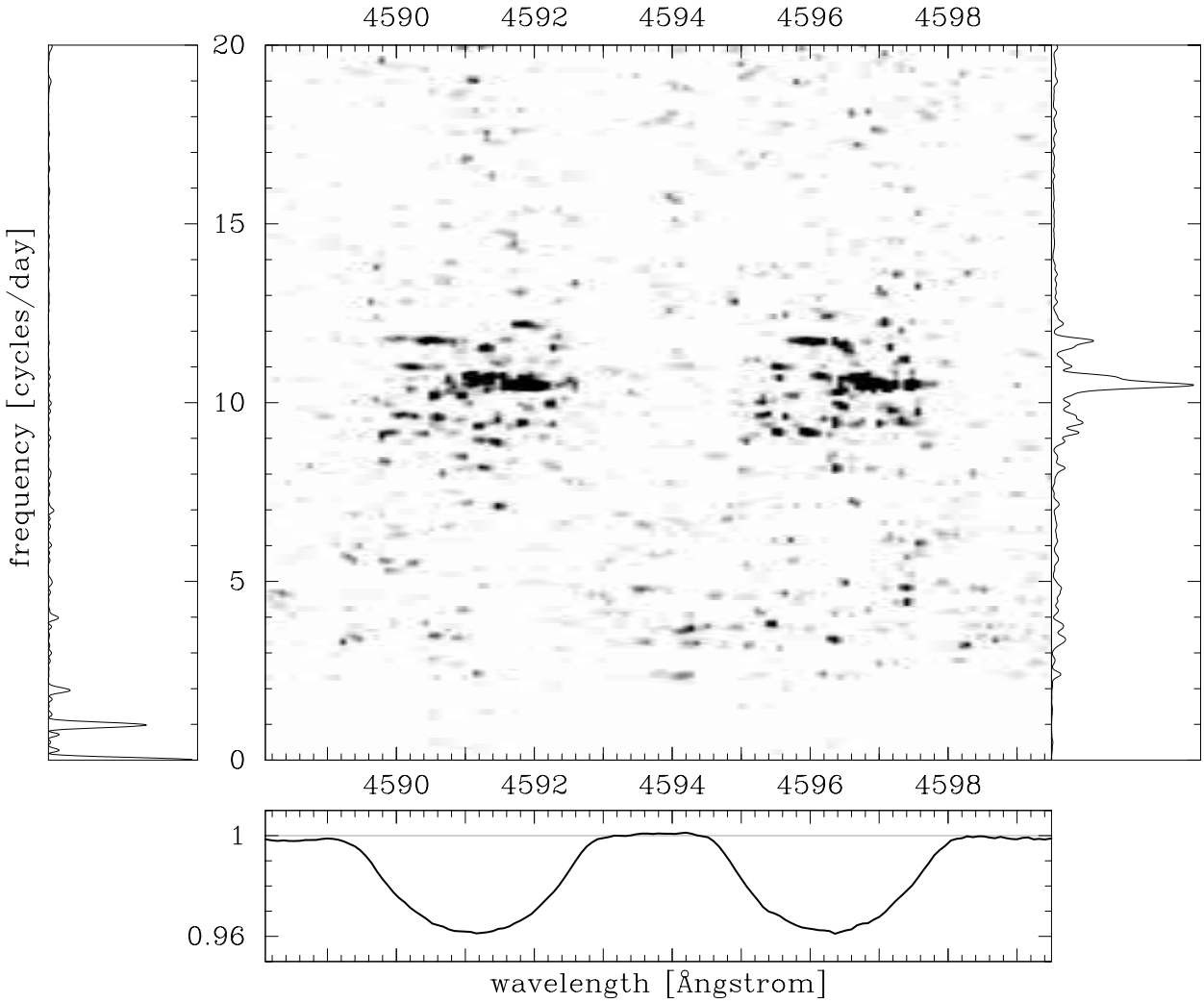

Fig. 4. CLEANed periodogram of the wavelength region of the O II 4590.8 and 4596.2 Å lines, with the corresponding summed periodogram in the right panel. The bottom panel shows the mean of the 78 spectra used to compute this periodogram; the left panel shows their window function. The signal was prewhitened for the orbital frequency and its first four harmonics. The double peak at 10.6 c/d, with its one-day aliases, is due to non-radial pulsations.

assumed, or that the primary is less massive than 13 $M_\odot$ which would imply $i \gtrsim 62°$.

5. Non-radial pulsations in the primary

We have analysed the line-profile variations of some of the absorption lines in the spectra of the primary of ψ^2 Ori, focussing on lines that are least affected by blending. We have tried to analyse some He I lines (4387, 5015, and 5047 Å), but found that the relatively strong, broad and moving profile of the secondary leads to inaccuracies in the analysis. These lines show orbital-phase dependent normalization errors, leading to Fourier spectra dominated by the orbital frequency and its first eleven (or so) harmonics. We found that for the absorption lines of heavier elements we had to prewhiten the data with the orbital frequency and its first four harmonics, in order to diminish the effects of the orbit. By doing so, however, we lose the ability to study line-profile variations of the primary that have frequencies similar to that of the orbit. The spectra and periodograms we discuss below all have these five frequencies removed.

In Fig. 1 we display the line-profile variations of the 4552 Å Si III line in different stages of the analysis. One can clearly see a moving bump pattern remeniscent of that of non-radial pulsations. After shifting the spectra to the velocity frame relative to the primary, it is evident that the bump pattern is not constant. The distance between consecutive bumps varies; beating of two similar moving-bump patterns seems present. This indicates that probably more modes than just one pulsation mode are responsible for the profile variations. The profiles of all other investigated absorption lines show variations very similar to those in the 4552 Å profile.

To study the temporal behaviour of the line-profile variations we have analysed them in the way described by Gies & Kullavanijaya (1988) and Telting & Schrijvers (1997). Figure 4 displays the periodogram resulting from

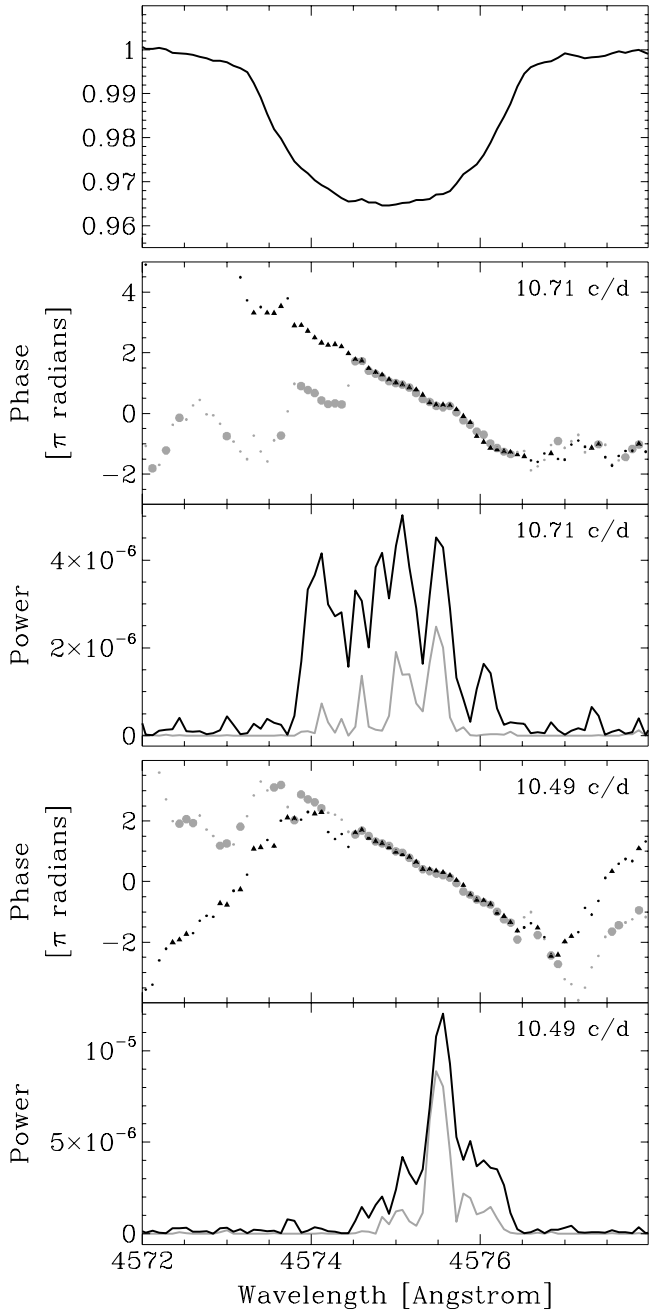

Fig. 5. Power and phase diagram of frequencies 10.49 and 10.71 c/d in the wavelength region of the Si III 4574 Å line. The black line (power) and the triangles (phase) represent the diagnostics as derived from the multi-sinusoid fit. The grey line and the circles are from the CLEANed periodogram. Phases are plotted as small dots for bins with insignificant power values. The top panel displays the mean spectrum.

CLEANing the Fourier transform (Roberts et al. 1987) of the signal in each wavelength bin in the profiles of the 4590 and 4596 Å O II lines. We used 400 CLEAN iterations with a gain of 0.2. A double power peak is found at frequency 10.5 c/d; the duplicity of this peak explains the apparent beating of the moving-bump pattern. One-day aliasing is still present in the periodogram; the CLEAN algorithm has not been able to fully correct for the window function.

Table 3. Observed frequencies in c/d and blue-to-red phase differences in π radians, of spectral line variations in ψ^2 Ori.

	C II 4267	Si III 4552	Si III 4567	Si III 4574	O II 4590	O II 4596
f_1	10.46	10.48	10.47	10.49	10.48	10.48
$\Delta\Psi$	3.0	3.5	3.5	4.8	3.9	4.5
f_2	10.73	10.76	10.74	10.71	10.73	10.73
$\Delta\Psi$	4.1	5.1	4.7	4.9	4.8	4.5

We have tried to resolve the two frequencies responsible for this double peak by first prewhitening the data with the frequency of the combined peak (10.5 c/d) and then redoing the Fourier analysis, in order to find the frequency of the lower-amplitude peak of the double peak. We find this peak to be at ∼10.73 c/d (see Table 3). Then we prewhitened the original signal with this frequency, and did a Fourier analysis to recover the frequency of the higher-amplitude peak of the double peak: ∼10.48 c/d (Table 3). Note that the HWHM of the main peak of the window function is 0.083 c/d, which means that our frequency resolution is about 0.17 c/d, corresponding to a time base of the observations of 6 days.

The amplitude and phase of the variations with the above two frequencies, as a function of position in the line profiles, give information about the pulsations that are responsible for these variations. We have analysed the amplitude and phase diagrams as obtained from the CLEANed periodogram, as well as those obtained from multi-sinusoid fits (in this case two sinusoids) to the data in each wavelength bin. For the multi-sinusoid fits we used the frequencies as derived from the CLEAN analysis (as listed in Table 3), and created amplitude and phase diagrams from the fitted amplitudes and phases (see our forthcoming paper on ν Cen, Schrijvers & Telting, for a further description of this method). In Fig. 5 we plot the resulting amplitude and phase diagrams for the Si III 4574 Å line. As the multi-sinus method is not affected by one-day aliasing, higher power is found than in the case of the CLEANed periodogram in which power has leaked to one-day aliases. From the overplotted phase diagrams we have determined the blue-to-red phase differences $\Delta\Psi$, which are a measure of the degree ℓ of the modes (see Telting & Schrijvers 1997). The resulting phase differences are listed in Table 3.

We use the linear representation for modes with $\ell - |m| < 6$ from Telting & Schrijvers (1997), $\ell = 0.015 + 1.109\Delta\Psi$ with $\Delta\Psi$ expressed in π radians, to derive the degree of the modes. For this representation the chance of correctly identifying the modal degree within an interval of $\ell \pm 1$ is about 84%.

In most lines the amplitude of the 10.48 c/d frequency was not detected in the blue wing. For this reason the phase diagram spans only about 75% of the total line width, which means that the derived values of $\Delta\Psi$ are lower limits for the ℓ value of the responsible mode.

The amplitude of the 10.73 c/d frequency is more symmetrically distributed over the line profiles. From general line-profile modelling it has become clear that the phase diagrams run along beyond $v \sin i$ of the star, albeit with low corresponding amplitude. As our dataset does not provide the accuracy to measure the full extent of the phase diagrams, the derived ℓ values will be lower limits.

Taking the largest values of $\Delta\Psi$ from Table 3 we find $\ell = 5.3$ for the 10.48 c/d frequency, and $\ell = 5.7$ for the 10.73 c/d frequency. Given the fact that our determinations are likely to be lower limits, we estimate the true value for both modes to be $\ell = 6$. In Fig. 5 one can see that the slope of the phase diagrams of both frequencies is very similar, which supports the possibility of both modes having the same degree.

We stress that, because of the limited time base of our data set and the corresponding limiting frequency resolution, the derived phases of the variations at these frequencies might be affected by each other. More data, spanning a longer time base, are needed to confirm our mode identifications.

We did not find significant power at the harmonics of the frequencies derived above, which means that we cannot estimate the m-values of the modes directly from the Fourier analysis (Telting & Schrijvers 1997). It is likely that due to the limited sampling of the variational signal, and the phase smearing during the individual exposures, it has not been possible to detect the harmonic variability in our dataset.

6. Discussion

It is interesting to investigate if the apparent frequencies of the two non-radial pulsations modes in the primary of ψ^2 Ori can shed some light on the question whether these modes are powered by tidal forces or from within the star.

6.1. Pulsation modes powered by tidal forces?

In a binary star, the perturbing force due to its companion star is periodic. Depending on the proximity of the orbit and on its eccentricity this periodic force is more or less sinusoidal, and can be expanded in a Fourier series in terms of the orbital frequency $\Omega_{\rm orb}$ (see e.g. Ruymaekers 1992; Smeyers et al. 1998). The perturbing frequencies as experienced by a mass element in the frame corotating with the star can be described as

$$\sigma_{\rm cor} = j\Omega_{\rm orb} + m\Omega_{\rm rot} \qquad (1)$$

with j a positive integer indicating harmonic $j-1$ of the orbital frequency, and with $\Omega_{\rm rot}$ the rotation frequency of the star. This means that for a non-sinusoidal perturbing force the star experiences a spectrum of frequencies of which some may coincide with an eigenfrequency such that resonances occur.

The apparent pulsation frequency of a resonance mode as seen by an observer depends on the azimuthal order m of the mode and the rotation frequency of the star

$$\sigma_{\rm obs} = \sigma_{\rm cor} - m\Omega_{\rm rot} = j\Omega_{\rm orb} \qquad (2)$$

where the rotation frequency is positive by definition and where negative m values represent prograde pulsation modes. Hence, if the pulsations are tidally induced, the observed pulsation frequencies should be multiples of the orbital period (Eq. (2)).

This binary has a very accurately determined orbital period, leading to $\Omega_{\rm orb} = 0.395889$ c/d. Taking the HWHM of the main peak of the window function, 0.083 c/d, as an estimate of the error in our frequency determinations, we find that the observed 10.73 c/d pulsation frequency is consistent with an integer value of j in Eq. (2): $j = 27.1 \pm 0.2$. However, the strongest detected frequency, 10.48 c/d, is inconsistent with an integer value of j: $j = 26.5 \pm 0.2$.

We conclude that given the observed frequencies it is unlikely that both detected pulsations in the primary of ψ^2 Ori are due to tidal forcing. However, it is clear that we need much more precise determinations of the pulsation frequencies in order to provide a conclusive answer. More high S/N spectra taken on a long time base are needed in order to achieve this.

6.2. Pulsation modes excited internally?

Here we investigate if the observed pulsation frequencies are consistent with those expected for internally excited β Cephei oscillations. Dziembowski & Pamyatnykh (1993) present the pulsation frequencies of modes with low and intermediate degree ℓ in an $M = 12\ M_\odot$ star. They present dimensionless frequencies in the corotating frame of the star, and hence for comparison we need to transform the observed frequencies using Eq. (2), assuming $m = -6$ and $\Omega_{\rm rot} = \Omega_{\rm orb}$. To transform to dimensionless frequencies we assume the radius and mass of the primary in ψ^2 Ori to be $R = 5.4\ R_\odot$ and $M = 13.9\ M_\odot$ (for inclination $i = 60°$).

The result of the above estimation is that the observed pulsation frequencies correspond to the lower limit of the unstable p-mode regime. If the observed modes are not sectoral, and hence $m > -6$, the transformation of Eq. (2) shifts the observed frequencies further into the p-mode regime. A similar conclusion was drawn for the observed $\ell \sim 9$ pulsation mode in the early-B type star ω^1 Sco (Telting & Schrijvers 1998).

7. Conclusions

We have shown that the primary of the close binary ψ^2 Ori exhibits non-radial pulsations. From our time series of spectra we have derived two pulsation frequencies of modes with intermediate ℓ values.

Following the frequency considerations in the previous sections, we conclude that the observed frequencies

$f_1 = 10.48\,\mathrm{c/d}$ and $f_2 = 10.73\,\mathrm{c/d}$ are consistent with internally excited p-mode β Cephei oscillations, and that it is unlikely that tidal forcing plays a dominant role for these modes. We stress, however, that more data is needed to confirm the pulsation frequencies, from which the above results were derived.

The observed ellipsoidal variations in ψ^2 Ori must be due to deformations due to equilibrium tide or dynamical tide with $\ell = 2$ behaviour. These should lead to apparent frequencies in the line-profile time series of low multiples of the orbital frequency. However, as indicated in Sect. 5, the fact that the line profiles of the two binary components cross also gives rise to orbital harmonics in the profile series. In our analysis it is difficult to disentangle these from the effect of tidal deformation. In order to investigate such deformations spectroscopically, one may try a dedicated technique to disentangle the spectra of double-lined spectroscopic binaries (Hadrava 1995) before attempting a frequency analysis on the line-profile variability.

Waelkens & Rufener (1983) suggested that for the closest binaries tidal interactions have a damping effect on β Cephei oscillations. The case of ψ^2 Ori provides evidence that this suggestion is not always true.

Acknowledgements. The authors wish to acknowledge the referee, Dr. C. Aerts, and Dr. B. Willems for their valuable comments.

J.A. would like to acknowledge John Telting for being a great supervisor and a good friend. He would also like to thank Johan Knapen for arranging the placement year at the ING, and Dr. A. Batten for his remarks regarding his work on the apsidal motion of ψ^2 Ori. Financial support is acknowledged from the Isaac Newton Group of Telescopes.

C.S. thanks John Telting and Saskia Prins for their hospitality in the days prior to the observing run.

References

Abt, H. A., & Levy, S. G. 1978, ApJS, 36, 241
Ashoka, B. N., & Padmini, V. N. 1992, Ap&SS, 192, 79
Batten, A. H., Fletcher, J. M., & Mann, P. J. 1978, Pub. Dominion Astrophys. Obs., 15, 121
Balona, L. A., & Dziembowski, W. A. 1999, MNRAS, 309, 221
Beardsley, W. R. 1969, Pub. Allegheny Obs., 8, 7
De Cat, P., Telting, J. H., Aerts, C., & Mathias, P. 2000, A&A, 359, 539
Chapellier, E., Le Contel, J. M., Le Contel, D., Sareyan, J. P., & Valtier, J. C. 1995, A&A, 304, 406
Chopinet, M. 1953, J. Obs., 44, 263
Claret, A., & Giménez, A. 1992, A&AS, 96, 255
Claret, A., & Giménez, A. 1993, A&A, 277, 487
Dziembowski, W. A., & Pamyatnykh, A. A. 1993, MNRAS, 262, 204
Gies, D. R., & Kullavanijaya, A. 1988, ApJ, 326, 813
Giménez, A. 1985, ApJ, 297, 405
Hadrava, P. 1995, A&AS, 114, 393
Hill, G. 1967, ApJS, 14, 263
Holmgren, D., Hadrava, P., Harmanec, P., Koubsky, P., & Kubat, J. 1997, A&A, 322, 565
Hutchings, J. B., & Hill, G. 1971, ApJ, 167, 137
Jerzykiewicz, M. 1984, Acta Astron., 34, 409
Kopal, Z. 1959, Close binary systems, London, UK
Kopal, Z. 1978, Dynamics of close binary systems (Dordrecht), The Netherlands
Lu, W. 1985, PASP, 97, 428
De Mey, K., Aerts, C., Waelkens, C., & Van Winckel, H. 1996, A&A, 310, 164
De Mey, K., Aerts, C., Waelkens, C., et al. 1997, A&A, 324, 1096
Monet, D. G. 1980, ApJ, 237, 513
Pearce, J. A. 1953, PASP, 65, 209
Percy, J. R. 1969, J. R. Astron. Soc. Canada, 63, 233
Plaskett, J. S. 1908, ApJ, 28, 266
Roberts, D. H., Lehár, J., & Dreher, J. W. 1987, AJ, 93, 968
Ruymaekers, E. 1992, A&A, 259, 349
Schrijvers, C., Telting, J. H., Aerts, C., Ruymaekers, E., & Henrichs, H. F. 1997, A&AS, 121, 343
Smith, M. A. 1985, ApJ, 297, 206
Smeyers, P., Willems, B., & Van Hoolst, T. 1998, A&A, 335, 622
Stairs, I. H., Arzoumanian, Z., Camilo, F., et al. 1998, ApJ, 505, 352
Tarasov, A. E., Harmanec, P., Horn, J., et al. 1995, A&AS, 110, 59
Telting, J. H., & Schrijvers, C. 1997, A&A, 317, 723
Telting, J. H., & Schrijvers, C. 1998, A&A, 339, 150
Warren, W. H., & Hesser, J. E. 1978, ApJS, 36, 497
Waelkens, C., & Rufener, F. 1983, A&A, 121, 45
Witte, M. G., & Savonije, G. J. 1999, A&A, 350, 129
Wolf, M., Diethelm, R., & Šarounová, L. 1999, A&A, 345, 553
De Zeeuw, P. T., Hoogerwerf, R., de Bruijne, J. H. J., Brown, A. G. A., & Blaauw, A. 1999, AJ, 117, 354